Remote Sensing and Mapping of Fine Woody Carbon With Satellite Imagery and Super Learner

Riyaaz Uddien Shaik, Mohamad Alipour, Eric Rowell, Adam Watts, Christopher Woodall, and Ertugrul Taciroglu

***Abstract*— Deadwood is a critical component of forest ecosystems, storing nutrients for plants and serving as a carbon store and emission source. Climate change influences forest ecosystem dynamics with the potential for deadwood to emit carbon more rapidly due to accelerated decay and increased wildfires and increased inputs via mass forest mortality and disturbance events. To objectively inform our understanding of wildfires and associated carbon emissions, this study estimates the carbon content of dead fine woody debris (FWD) using multimodal data, such as Landsat-8 multispectral imagery, Sentinel-1 (C-band) and PALSAR (L-band) synthetic aperture radar (SAR) imagery, and terrain features to estimate the FWD of less than 0.25 in (1 h), 0.25–1 in (10 h), and 1–3 in (100 h). This data fusion provides spectral information to assess vegetation health that correlates with deadwood, as well as penetrability from SAR, resulting in structural information and biomass sensitivity. An ensemble machine learning (ML) model was trained using measurements from the Forest Inventory and Analysis (FIA) Database. A feature importance analysis was also performed to investigate the importance of input features to the model's performance. A super learner regression (SLR) model composed of 9 base learners, including an ElasticNet model as meta-learner, was proposed and achieved the R^2 values of 0.75, 0.72, and 0.62 to estimate 1-, 10-, and 100-h FWD, respectively. The validated model was then used to estimate deadwood carbon in the 2021 Dixie Fire region of California, demonstrating the effectiveness of our approach, emphasizing the value of multimodal data for real-time FWD carbon stock estimation.**

***Index Terms*— Carbon stock, ensemble model, machine learning (ML), remote sensing.**

I. INTRODUCTION

DOWNED dead wood (DDW) encompasses detrital elements within forest ecosystems, comprising individual pieces across a range of sizes from the smallest twigs and branches rapidly consumed in fires [i.e., fine woody debris (FWD)] to the largest fallen trees (i.e., coarse woody debris). These DDW components play crucial roles in the structure and functioning of forest ecosystems, serving as wildlife habitats, drivers of fire behavior, stores of carbon, and providers of nutrients [1]. In recent decades, there has been a growing recognition of the multifaceted influence of DDW on various ecological characteristics and processes, especially related to carbon storage. Due to its relatively slow decomposition rate, DDW serves as a significant long-term carbon storage reservoir [2]. It is estimated that dead organic matter constitutes about 14% of the carbon stock in the U.S.'s forests [3]. However, the amounts of dead wood vary considerably between different types of forests and even within them [4]. Large accumulations of DDW are often the result of disturbances, such as wind, snow, ice, and disease. With the anticipation of increased frequency and severity of these disturbances due to global change [5], it is expected that the rates of tree mortality and, consequently, inputs of DDW carbon to forest ecosystems will also rise, but with potential increased emissions due to wildfires and accelerated decay [6].

Despite its significant ecological role and implications for forest management, DDW has often been overlooked, in part due to its lack of commercial value and the expenses and challenges associated with measuring it. As a signatory to the United Nations Framework Convention on Climate Change, the United States provides an annual carbon estimate for the forest sector that includes DDW [7]. The growing interest in DDW has prompted improved efforts to quantify it through field surveying under the U.S. Forest Service's Forest Inventory and Analysis (FIA) Program [8]. The FIA program has been instrumental in field surveying and compiling the most comprehensive database on various forest characteristics and health indicators [8] despite the challenges and costs of collecting FWD data. While there has been increased research attention to the use of artificial intelligence (AI) for estimating canopy biomass ([9] as a recent example), to the best of authors' knowledge, there is substantially less published DDW carbon stock analyses relative to live tree carbons using globally available spaceborne data. Therefore, in this study, we aim to develop a procedure for estimating FWD carbon stocks by leveraging globally available remote sensing data and machine learning (ML) techniques. FWD

Received 1 August 2024; revised 24 October 2024; accepted 6 November 2024. Date of publication 20 November 2024; date of current version 4 December 2024. The work of Riyaaz Uddien Shaik and Ertugrul Taciroglu was supported by Edison International. *(Corresponding author: Riyaaz Uddien Shaik.)*

Riyaaz Uddien Shaik and Ertugrul Taciroglu are with the Department of Civil and Environmental Engineering, University of California Los Angeles, Los Angeles, CA 90095 USA (e-mail: riyaaz@ucla.edu; etacir@ucla.edu).

Mohamad Alipour is with the Department of Civil and Environmental Engineering, the Grainger College of Engineering, University of Illinois Urbana-Champaign, Champaign, IL 61801 USA (e-mail: alipour@illinois.edu).

Eric Rowell is with the School of Environmental and Forest Sciences, University of Washington, Seattle, WA 98195 USA (e-mail: erowel@uw.edu).

Adam Watts is with the USDA Forest Service Pacific Wildland Fire Sciences Laboratory, Seattle, WA 98103 USA (e-mail: adam.watts@usda.gov).

Christopher Woodall is with the USDA Forest Service Northern Research Station, Durham, NH 03824 USA (e-mail: christopher.w.woodall@usda.gov).

Digital Object Identifier 10.1109/LGRS.2024.3503585

TABLE I
INDICES USED AS TRAINING FEATURES

Index	Formula	Source	Application	Ref.
Normalized Difference Veg. Index (NDVI)	$\frac{NIR-R}{NIR+R}$	L8	Vegetation dynamics	[9]
SAR Ratio (SR-1)	$\frac{VH}{VV}$	S1	Vegetation separability	[12]
SAR Ratio (SR-2)	$\frac{VV}{VH}$	S1	Surface vegetation growth	[13]
Power Ratio (PR)	$\frac{\lvert VV\rvert^2_{\text{dB}}}{\lvert VH\rvert^2_{\text{dB}}}$	S1	Land cover classification	[14]
Total Scattering Power (SPAN)	$\frac{1}{2}(\lvert VV\rvert^2 + \lvert VH\rvert^2)$	S1	Land cover classification	[14]
Difference Intensity (DI)	$\frac{1}{2}(\lvert VV\rvert^2 - \lvert VH\rvert^2)$	S1	Land cover classification	[14]
Radar Vegetation Index (RVI)	$\frac{4xVH}{VV+VH}$	S1	Vegetation & bare soil separability	[15]
C-band Normalized Polarized Diff (C-NPDI)	$\frac{VV-VH}{VV+VH}$	S1	Vegetation optical depth	[16]
L-band Normalized Polarized Diff (L-NPDI)	$\frac{VV-VH}{VV+VH}$	PL	Vegetation optical depth	[16]
Estimation of Signal Parameters via Rotational Invariance Techniques (ESPRIT)	$\frac{HH+HV}{2}$	PL	Sensitive to vegetation height	[17]
L-band Difference (L-DIFF)	$HH - HV$	PL	Sensitive to vegetation height	[18]
C-band Ratio (C-Ratio)	$\frac{HH}{HV}$	PL	Sensitive to vegetation height	[18]

consists of various forest ecosystem inputs of dead wood from branch shedding and plant mortality, which are divided into three size classes ascribed to categories based on the time roughly needed to influence their moisture characteristics needed for fire behavior modeling input collectively known as time lags: 1 h (FWD1), 10 h (FWD10), and 100 h (FWD100). These classifications correspond to diameters ranging from less than one-fourth inch, one-fourth to one inch, and one to 3 in, respectively [1]. With the increasing use of AI-based algorithms in remote sensing and forest management, the FIA data are being utilized for new applications as a valuable resource for model training and knowledge extraction [9], [10].

This letter introduces an ML-based framework that integrates multiple satellite data modalities and employs a super learner regression (SLR) model, which is a combination of ensemble and stacked ML models trained on FIA's georeferenced FWD1, FWD10, and FWD100 data for estimating FWD carbon stocks. Furthermore, the 2021 Dixie Fire region was selected to demonstrate the ability of our model to estimate FWD carbon stock release due to wildfire events.

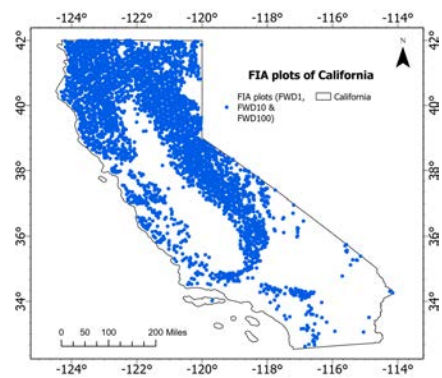

Fig. 1. Outline depicting the area of study (California) and points representing FIA plots with assigned FWD biomass (FWD1, FWD10, and FWD100) (locations here are approximate to maintain FIA spatial confidentiality).

II. STUDY AREA

This study selected California as the focal region for data collection and modeling. Fig. 1 illustrates the geographical scope of the study area and the specific fuel plots used. Spanning elevations from −86 m in Death Valley to 4421 m at the summit of Mt. Whitney, California, boast diverse topography. Approximately 40% of the total land area of the state, which is approximately 13.35 million hectares, is covered by forests [11]. California's ecosystems include alpine, montane, and subalpine forests, coastal forests, mixed conifer-deciduous forests, chaparral, pinyon-juniper woodlands, and desert scrub. The state's extensive range of forest types and susceptibility to wildfires make it an ideal subject for this research.

III. DATA UTILIZED

The input variable array was crafted to incorporate remote sensing indices that correlate with vegetation and land cover characteristics, informed by prior research, as presented in Table I. These inputs for the SLR model were derived from a synthesis of four distinct open source remote sensing datasets, comprising Landsat-8 (L8) optical imagery, Sentinel-1 (S1) C-band synthetic aperture radar (SAR) data, phased array-type L-band synthetic aperture radar (PALSAR) data, as well as shuttle radar topography mission (SRTM) elevation and slope data. The multispectral data from Landsat are effective for observing visual information, such as the color, texture, and photosynthetic activity estimation of vegetation, helping in identifying species, health status, and density of the forest. C-band SAR can penetrate moderate density canopy cover and provide data regardless of cloud cover or light conditions. This frequency band is sensitive to moisture content in vegetation. L-band has a longer wavelength compared with the C-band, allowing it to penetrate deeper into the canopy and even the forest understory. This characteristic makes L-band important for estimating surface forest biomass. We created vegetation indices using these datasets, which will be explained in the following sections. L8 (NIR and red bands), S1 (VV and VH bands), PALSAR (HH and HV bands), and SRTM (DEM) datasets were accessed through the Google Earth Engine

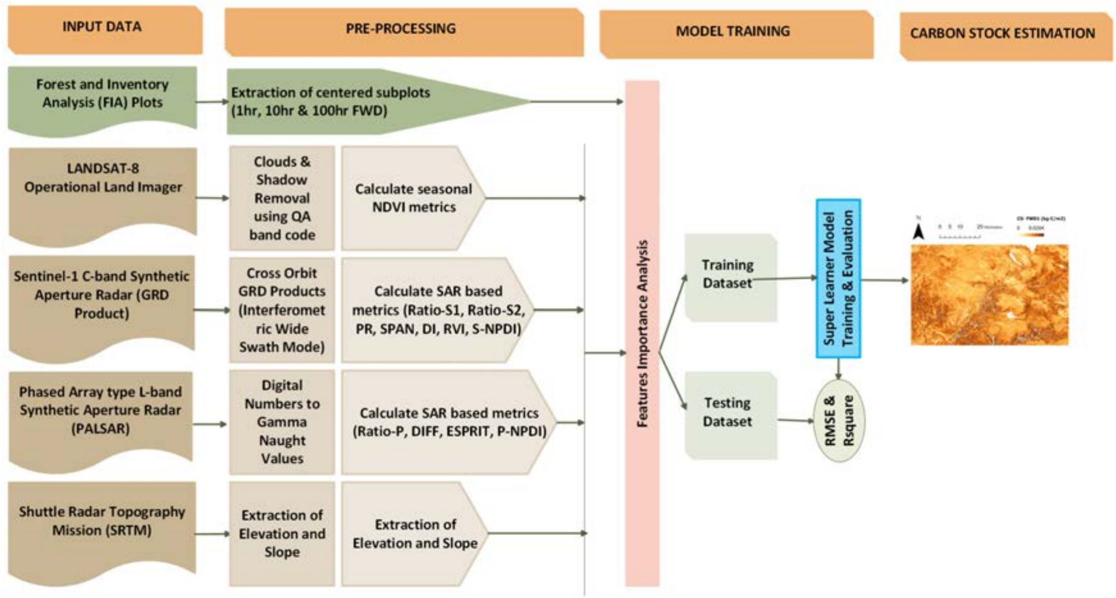

Fig. 2. Carbon stock estimation for time-lag FWD framework.

(GEE) platform and merged at varying spatial and temporal resolutions to produce individual arrays, each approximating a spatial resolution of 30 × 30 m.

The FIA program conducts a comprehensive inventory of forests across the United States, serving as the primary initiative for gathering, publishing, and analyzing data regarding forest land ownership [19]. Its spatial sampling method involves approximately one plot per 6000 acres. One of the key indicators provided by FIA is the assessment of DDW, which offers crucial estimates regarding the presence and density of down and dead woody materials. These estimates play a significant role in evaluating various forest attributes, including carbon stocks, fuel loadings, and structural diversity. According to FIA's definition, DDW encompasses a range of materials, such as fine and coarse woody debris, slash piles, duff, and litter, as well as the cover and height of shrubs and herbs. Fig. 1 displays the distribution of DDW data measured in the field for California, sourced from FIA plots spanning from 2015 to 2019 [19]. Satellite imagery corresponding to the timeframe of 3461 FIA plots from 2015 was collected and incorporated into a tabular dataset, which was then divided into training (80%) and testing (20%) datasets.

IV. Methodology

In this section, we introduce a concise flowchart, depicted in Fig. 2, illustrating the step-by-step methodology of our research.

First, we ensured the relevance and quality of input data through meticulous collection and curation. Second, a preprocessing step was employed to clean and standardize the data, which involved calculating various indices and merging cross-orbit data for S1. Third, we conducted feature importance analysis using permutation importance [20] to understand the impact of each feature on model performance. This process involved shuffling the values of individual predictor features and then re-evaluating model accuracy with the modified data knowing that shuffling more important features will damage model performance more severely. The significance of each feature was assessed by comparing the baseline accuracy with the decrease in accuracy resulting from shuffling the feature values. An examination of the importance scores of all features revealed that NDVI from L8, ESPRIT derived from PALSAR, and HV from PALSAR and elevation from SRTM stood as important features. This is consistent with other studies, as the L8-based feature takes advantage of the strong spectral contrast between the NIR and red bands [21]. PALSAR-based L-band features have the ability to interact with structural constituents due to their longer wavelengths [22], and elevation influences the density of deadwood [23], whereas SR-1, SR-2, and RVI derived from S1 exhibited negative scores to four decimal places due to reduced proportion of surface scattering. Despite excluding these features from the model during retraining, the accuracy remained unchanged, indicating that C-band features have little influence on model performance and can be retained within the model [24]. Fourth, determining the most suitable learner for a particular dataset and prediction task beforehand is challenging. The SLR model addresses this challenge by considering a broad range of user-specified algorithms, ranging from parametric regressions to nonparametric ML algorithms [25]. This approach mitigates concerns about selecting a single "right" algorithm and allows for leveraging the strengths of a diverse set of ML models and in capturing diverse ecosystem gradients [10]. We implemented an SLR ensemble model [25], including the nine base learners: support vector machine (SVR), decision tree (DT), K-nearest neighbors (kNNs), AdaBoost regressor (AR), bagging regressor (BR), random forest (RF), extra trees regressor (ER), gradient boosting method (GBM), and XGBoost regression (XR). We selected ElasticNet (EN), an extended linear regression model, as the meta-learner in

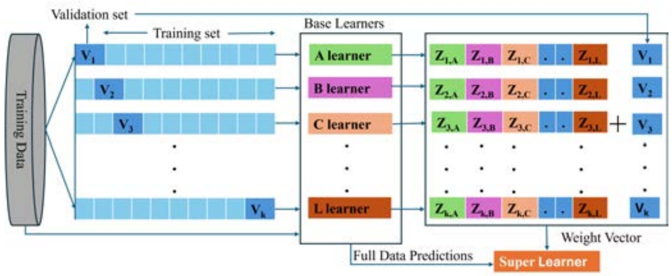

Fig. 3. Overall procedure of the SLR model.

this approach. The SLR model was trained using FIA's FWD1, FWD10, and FWD100 data. Hyperparameter optimization was performed using automated ML optimization capabilities, such as the skopt Python library, on an NVIDIA GeForce RTX 3070 GPU, which minimized overfitting and enhanced system performance. Fig. 3 illustrates the overall procedure of the SLR model. Fifth, the trained model underwent a rigorous evaluation to assess its accuracy using root-mean-square error (RMSE) and R^2 and effectiveness in capturing underlying data patterns. Sixth, subsequently, the trained model was utilized to generate biomass maps for FWD1, FWD10, and FWD100 for the selected region of interest. Seventh, estimating the carbon storage of FWD involves calculating the product of volume, density, and carbon concentration. Harmon et al. [26] compiled literature values for carbon concentrations in dead woody debris. Due to the lack of carbon concentration data for many species, the FIA database used in this study adopts average values: 49% for hardwoods, 52% for softwoods, and 51% for unknown species types. It should be noted that while a recent study by Martin et al. [27] on carbon conversion has slightly revised dead wood carbon content to 48%, this study applied the averages in the database to convert the generated biomass maps for FWD1, FWD10, and FWD100 into carbon stock maps, CS1, CS10, and CS100, respectively. The flowchart in Fig. 2 provides a coherent and systematic overview of our methodology.

V. Results and Discussion

In this section, we provide an assessment of the trained SLR model and demonstrate carbon stock maps for a prefire region, demonstrating the efficacy of our methodology in accurately identifying fine wood carbon stocks. We assessed the SLR model using a testing dataset for FWD1, FWD10, and FWD100, yielding the RMSE and R^2 values of 0.004 kg/m^2 and 0.75, 0.012 kg/m^2 and 0.72, and 0.150 kg/m^2 and 0.62, respectively, as depicted in Fig. 4(a), (c), and (e). Previously, D'Este et al. [28] conducted research to estimate FWD1 and obtained best R^2 as 0.50 with the RF model. Through the collective intelligence of multiple models, our architecture adeptly generalizes and predicts outcomes with precision and robustness to diverse data patterns and complexities. To the best of the authors' knowledge, this work is the first to model FWD10 and FWD100 estimations using data only from spaceborne sensors.

It can be seen that performance degrades with an increase in particle size. This trend can be associated with differences in

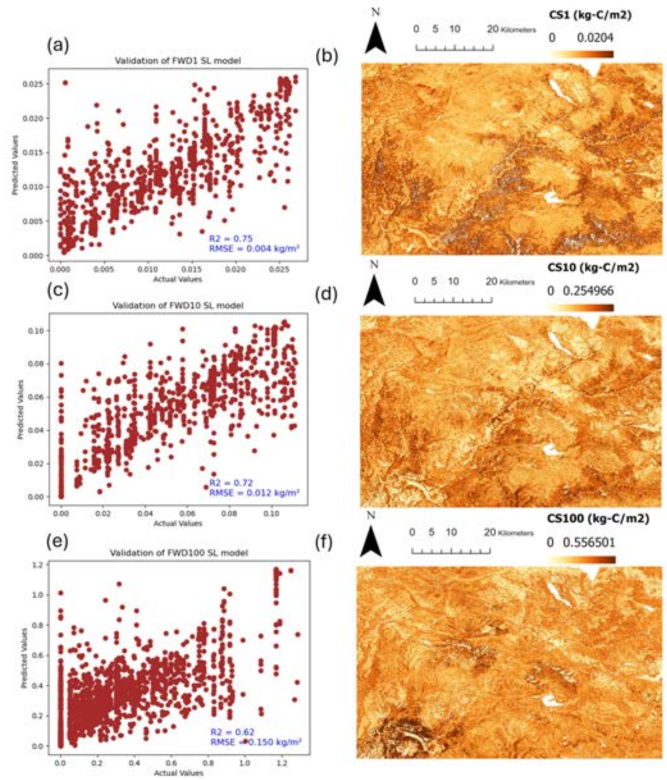

Fig. 4. (a), (c), and (e) Plots showing predicted versus actual biomass estimations for FWD1, FWD10, and FWD100. (b), (d), and (f) Time-lag (CS1, CS10, and CS100) carbon stock estimations for Dixie Fire region.

the underlying drivers of woody debris of different sizes [29]. Recent work has hypothesized that finer woody debris may be more related to crown plasticity and minor disturbances, while coarser debris may be driven by major mortality events [30]. Integrating disturbances in modeling FWD and testing these hypotheses is beyond the scope of this letter and should be the subject of future work. Overall, given the complexity of the problem, our performance evaluation demonstrates acceptable model learning behavior and illustrates the feasibility of the approach for wider future application.

Subsequently, we utilized the trained SLR model to develop prefire carbon stock maps for a selected case study area, encompassing regions affected by the Dixie Fire, which ignited on July 13, 2021, and it stands as one of the largest documented wildfires to date, scorching an area of 374 000 hectares [31]. Our CS1, CS10, and CS100 maps are visualized in Fig. 4(d), (e), and (f), respectively, and each row in Fig. 4 was created by a model separately trained to estimate the respective FWD category for the entire area of study. Fine wood carbon stocks (CS1, CS10, and CS100) for this region accounted for 0.004, 0.01, and 0.06 t-C/ha, respectively, and the total fine wood carbon is 0.074 t-C/ha.

While the FIA data used in this study have proven exceptionally helpful for model training, Woodall and Lutes [32] have conducted a sensitivity analysis on the adequacy of FWD representation in this dataset. In particular, uncertainty in estimating the occurrence of small 1-hour fuel particles coupled with uncertainty regarding quadratic mean diameter assumptions [33] greatly influences the resulting fuel loading calculations for any given forest beyond that of many other aspects of the DDW inventory program. As a result, this uncertainty should be considered in practical applications with regards to the degree of quantitative accuracy required. Nevertheless, the FIA data remain a valuable resource for mapping and estimation of biomass and qualitative wildfire fuel characterization [10]. Furthermore, this study focused on carbon estimation in FWD, which is associated with crown plasticity and minor disturbances, whereas large-sized woody debris (i.e., coarse woody debris) is more closely related to higher intensity mortality events involving larger sized trees and associated branches. Therefore, future work may be needed to fully investigate the adequacy of the models for larger particles.

VI. Conclusion

The proposed methodology integrated multiple modalities of satellite data and AI, achieving the R^2 values of 0.75, 0.72, and 0.62 for carbon stocks CS1, CS10, and CS100, respectively. To showcase the capability of our SLR model, we applied it to the Dixie Fire region, producing prefire carbon stock maps for time-lag FWDs. Our SLR model, guided by geo-referenced labeled data, establishes a robust foundation for spatial carbon stock estimations.

Acknowledgment

The authors would like to thank Hans Anderson and John Chase of USDA Forest Services for providing the FIA data and helping interpret them. They would also like to thank Park Williams (Professor, Department of Geography, University of California, Los Angeles) for his review and helpful feedback.

References

[1] C. W. Woodall and G. C. Liknes, "Climatic regions as an indicator of forest coarse and fine woody debris carbon stocks in the United States," *Carbon Balance Manage.*, vol. 3, no. 1, pp. 1–8, Dec. 2008.

[2] J. L. Campbell et al., "Estimating uncertainty in the volume and carbon storage of downed coarse woody debris," *Ecol. Appl.*, vol. 29, no. 2, Mar. 2019, Art. no. e01844.

[3] Y. Pan et al., "A large and persistent carbon sink in the world's forests," *Science*, vol. 333, no. 6045, pp. 988–993, 2011.

[4] M. E. Harmon and C. Hua, "Coarse woody debris dynamics in two old-growth ecosystems," *BioScience*, vol. 41, no. 9, pp. 604–610, Oct. 1991.

[5] B. M. Wotton, "Climate change and forest disturbances," *Bioscience*, vol. 51, no. 9, pp. 723–734, 2001.

[6] B. J. Wijas et al., "The role of deadwood in the carbon cycle: Implications for models, forest management, and future climates," *Annu. Rev. Ecology, Evol., Systematics*, vol. 55, no. 1, pp. 133–155, Nov. 2024.

[7] H. S. Eggleston, L. Buendia, K. Miwa, T. Ngara, and K. Tanabe, "2006 IPCC guidelines for national greenhouse gas inventories," U.S. Dept. Energy Office Scientific Tech. Inf., Inst. Global Environ. Strategies, Kanagawa, Japan, Tech. Rep., 2006.

[8] C. W. Woodall et al., "The downed and dead wood inventory of forests in the United States," *Sci. Data*, vol. 6, no. 1, pp. 1–13, Jan. 2019.

[9] T. Chang, B. P. Rasmussen, B. G. Dickson, and L. J. Zachmann, "Chimera: A multi-task recurrent convolutional neural network for forest classification and structural estimation," *Remote Sens.*, vol. 11, no. 7, p. 768, Mar. 2019.

[10] R. U. Shaik, M. Alipour, E. Rowell, B. Balaji, A. Watts, and E. Taciroglu, "FUELVISION: A multimodal data fusion and multimodel ensemble algorithm for wildfire fuels mapping," 2024, *arXiv:2403.15462*.

[11] A. Bytnerowicz and M. E. Fenn, "Nitrogen deposition in California forests: A review," *Environ. Pollut.*, vol. 92, no. 2, pp. 127–146, 1996.

[12] X. Blaes, P. Defourny, U. Wegmuller, A. D. Vecchia, L. Guerriero, and P. Ferrazzoli, "C-band polarimetric indexes for maize monitoring based on a validated radiative transfer model," *IEEE Trans. Geosci. Remote Sens.*, vol. 44, no. 4, pp. 791–800, Apr. 2006.

[13] S. Koley and J. Chockalingam, "Sentinel 1 and Sentinel 2 for cropland mapping with special emphasis on the usability of textural and vegetation indices," *Adv. Space Res.*, vol. 69, no. 4, pp. 1768–1785, Feb. 2022.

[14] S. A. Sayedain, Y. Maghsoudi, and S. Eini-Zinab, "Assessing the use of cross-orbit Sentinel-1 images in land cover classification," *Int. J. Remote Sens.*, vol. 41, no. 20, pp. 7801–7819, Oct. 2020.

[15] S. Periasamy, "Significance of dual polarimetric synthetic aperture radar in biomass retrieval: An attempt on Sentinel-1," *Remote Sens. Environ.*, vol. 217, pp. 537–549, Nov. 2018.

[16] Z. Li, L. Ding, and D. Xu, "Exploring the potential role of environmental and multi-source satellite data in crop yield prediction across northeast China," *Sci. Total Environ.*, vol. 815, Apr. 2022, Art. no. 152880.

[17] D. Liu and Y. Wang, "Estimation of tree height using the ESPRIT algorithm with ALOS/PALSAR dual-pol InSAR datasets," in *Proc. 13th Eur. Conf. Synth. Aperture Radar*, Mar. 2021, pp. 1–4.

[18] W. Chen, Q. Zheng, H. Xiang, X. Chen, and T. Sakai, "Forest canopy height estimation using polarimetric interferometric synthetic aperture radar (PolInSAR) technology based on full-polarized ALOS/PALSAR data," *Remote Sens.*, vol. 13, no. 2, p. 174, Jan. 2021.

[19] E. A. Burrill, A. M. DiTommaso, J. A. Turner, S. A. Pugh, J. Menlove, G. Christiansen, C. J. Perry, and B. L. Conkling, "The forest inventory and analysis database: Database description and user guide version 9.0 for Phase 2," U.S. Dept. Agricult., Forest Service, Collins, CO, USA, Gen. Tech. Rep. RMRS-GTR-245, p. 1024, 2021. [Online]. Available: http://www.fia.fs.fed.us/library/database-documentation/

[20] L. Breiman, "Random forests," *Mach. Learn.*, vol. 45, pp. 5–32, Oct. 2001.

[21] M. L. Clark, D. A. Roberts, M. E. Gardner, and D. R. Weise, "Estimation of Hawaiian Islands fire fuel parameters from hyperspectral imagery," in *Proc. Airborne Earth Sci. Workshop*, 2004, p. 45.

[22] L. Naidoo et al., "The assessment of data mining algorithms for modelling Savannah woody cover using multi-frequency (X-, C- and L-band) synthetic aperture radar (SAR) datasets," in *Proc. IEEE Geosci. Remote Sens. Symp.*, Jul. 2014, pp. 1049–1052.

[23] I. C. Petritan, V.-V. Mihăilă, J. C. Yuste, O. Bouriaud, and A. M. Petritan, "Deadwood density, C stocks and their controlling factors in a beech-silver fir mixed virgin European forest," *Forest Ecology Manage.*, vol. 539, Jul. 2023, Art. no. 121007.

[24] L. Naidoo et al., "Savannah woody structure modelling and mapping using multi-frequency (X-, C- and L-band) synthetic aperture radar data," *ISPRS J. Photogramm. Remote Sens.*, vol. 105, pp. 234–250, Jul. 2015.

[25] R. V. Phillips, M. J. van der Laan, H. Lee, and S. Gruber, "Practical considerations for specifying a super learner," *Int. J. Epidemiology*, vol. 52, no. 4, pp. 1276–1285, Aug. 2023.

[26] M. E. Harmon, C. W. Woodall, B. Fasth, and J. Sexton, "Woody detritus density and density reduction factors for tree species in the United States: A synthesis," USDA Forest Service, Suite, PA, USA, Tech. Rep. NRS-29, 2008.

[27] A. R. Martin, G. M. Domke, M. Doraisami, and S. C. Thomas, "Carbon fractions in the world's dead wood," *Nature Commun.*, vol. 12, no. 1, p. 889, 2021.

[28] M. D'Este, M. Elia, V. Giannico, G. Spano, R. Lafortezza, and G. Sanesi, "Machine learning techniques for fine dead fuel load estimation using multi-source remote sensing data," *Remote Sens.*, vol. 13, no. 9, p. 1658, Apr. 2021.

[29] C. W. Woodall and A. R. Weiskittel, "Relative density of United States forests has shifted to higher levels over last two decades with important implications for future dynamics," *Sci. Rep.*, vol. 11, no. 1, p. 18848, Sep. 2021.

[30] C. W. Woodall, S. Fraver, S. N. Oswalt, S. A. Goeking, G. M. Domke, and M. B. Russell, "Decadal dead wood biomass dynamics of coterminous U.S. forests," *Environ. Res. Lett.*, vol. 16, no. 10, Oct. 2021, Art. no. 104034.

[31] A. H. Taylor, L. B. Harris, and C. N. Skinner, "Severity patterns of the 2021 dixie fire exemplify the need to increase low-severity fire treatments in California's forests," *Environ. Res. Lett.*, vol. 17, no. 7, Jul. 2022, Art. no. 071002.

[32] C. W. Woodall and D. C. Lutes, "Sensitivity analysis of down woody material data processing routines," United States Dept. Agricult. Forest Service, St. Paul, MN, USA, Tech. Rep. NC 35, 2005, vol. 352, p. 199.

[33] C. W. Woodall and V. J. Monleon, "Estimating the quadratic mean diameters of fine woody debris in forests of the united states," *Forest Ecol. Manage.*, vol. 260, no. 6, pp. 1088–1093, Aug. 2010.